ABSTRACT

Title of Document: VERIFICATION OF SHAFT FOUNDATION LRFD DESIGN USING FINITE ELEMENT METHOD

Kuang-Yuan Hou, Master of Science, 2017

Directed By: Research Professor Chung C. Fu

Department of Civil and Environmental Engineering

Shaft is used as a foundation to support mast arm signal pole structure and transfer load from superstructures to deeper firm strata. The capacity of current shaft foundation deployed in the State of Maryland is re-verified due to higher strength requirement against structural fatigue proposed from AASHTO LRFD Specification for Structural Supports for Highway Signs, Luminaries, and Traffic (2015). The primary object of this research is to evaluate the adequacy of the current shaft foundation design procedure. The shaft foundation verification includes embedment length, reinforcement concrete design based on moment and shear, and torsional capacity. For embedment length check, lateral reactions between soil and shaft are verified by comparing analytical method and finite element method. Wind-induced torque is a design concern for the shaft of a single pole structure. However, torsional capacity of the shaft foundation of signal pole structures is rarely mentioned in the current design specification. Therefore, by validating finite element models with analytical method, torsional effect is further simulated to the finite element model.

VERIFICATION OF SHAFT FOUNDATION LRFD DESIGN USING FINITE ELEMENT METHOD

By

Kuang-Yuan Hou.

Thesis submitted to the Faculty of the Graduate School of the
University of Maryland, College Park, in partial fulfillment
of the requirements for the degree of
Master of Science
2017

Advisory Committee:
Professor Chung C. Fu, Chair
Professor M. Sherif Aggour
Professor Brian M. Phillips

© Copyright by
Kuang-Yuan Hou
2017

Acknowledgements

I would like to express my gratefulness to Dr. Chung C. Fu, P.E., who has been advising me and guiding me through the development of this thesis. His insightfulness and encouragement are indispensable parts towards the completion of this thesis, and he helped me all the time during my graduate life in University of Maryland. I also thank Dr. Brian M. Philip, and Dr. M. Sherif Aggour, for serving my thesis committee. The knowledge I learned from their lectures is invaluable material facilitating me to complete this thesis. I am also deeply indebted to the BEST Center group members, Chaoran Xu, Yunchao Ye, Yifan Zhu, and visiting scholar Dr. Xinyi Huang who helped me in learning the ANSYS finite element program and provided me with important resource.

Table of Contents

Acknowledgements ii
Table of Contents iii
List of Tables iv
List of Figures v
List of Notations vi
Chapter 1: Introduction 1
1.1 Problem Statement and research motivation 1
1.2 Research Objective 2
1.3 Thesis Organization 3
Chapter 2: Literature review 4
2.1 Lateral soil reaction 4
2.2 Torsional capacity 10
Chapter 3: Analytical verification 14
3.1 Embedment length 14
3.2 Torsional Capacity 15
Chapter 4: Analytical verification for general soil in Maryland 20
4.1 Embedment length check 20
4.2 Reinforcement concrete design check 21
4.3 Torsional capacity check 24
Chapter 5: Finite element modeling 27
5.1 Finite element model design 27
5.2 Finite element model establishment 34
5.3 Finite element method analysis result 37
Chapter 6: Conclusion, Discussion, and Future work 47
6.1 Summaries and Conclusions 47
6.2 Future work 48
Bibliography 49

List of Tables

Table 2-1 Pile classification under laterally loaded (Broms 1964) 4
Table 2-2 p-y curve for soft clay (API 2005) 8
Table 2-3 Adherence factors for pile driving in stratified soils Tomlinson (1970) 11
Table 4-1 Assumed properties of soil for hypothetical cases 20
Table 4-2 Ground shear and moment (LRFD Strength I) 20
Table 4-3 Embedment length verification 21
Table 4-4 Standards for highways and incidental structures 22
Table 4-5 3'X10' shaft torsional capacity 25
Table 4-6 4'X10' shaft torsional capacity 26
Table 5-1 Finite element model parameter 27
Table 5-2 Assumed cohesive soil properties 27
Table 5-3 Assumed cohesionless soil properties 27
Table 5-4 Parameters for soil spring 30
Table 5-5 Cohesionless soil spring 33
Table 5-6 Cohesive soil spring 34
Table 5-7 Finite element model list 38
Table 5-8 FEM analysis result of lateral reaction 1.5D removed (cohesive) 39
Table 5-9 FEM analysis result of lateral reaction 0.75D removed (cohesive) 40
Table 5-10 FEM analysis result of lateral reaction non-removed (cohesive) 41
Table 5-11 FEM analysis result of lateral reaction (cohesionless) 43
Table 5-12 Three-dimensional analysis model 44
Table 5-13 3-dimension finite element analysis result in cohesive soil -0.75D removed 45
Table 5-14 3-dimension finite element analysis result in cohesive soil 1.5D removed 46
Table 5-15 3-dimension finite element analysis result in cohesionless soil 46

List of Figures

Figure 2-1 Short pile 5
Figure 2-2 Long pile 5
Figure 2-3 Single pile model (FHWA 2010) 7
Figure 2-4 Combined torsion and lateral loading (McVay et al. 2014) 13
Figure 4-1 P-M interaction curve for 50’ arm length signal structure 23
Figure 4-2 P-M interaction curve for 60’ arm length signal structure 23
Figure 4-3 P-M interaction curve for 70’ arm length signal structure 24
Figure 4-4 P-M interaction curve for 75’ arm length signal structure 24
Figure 5-1 2D model demonstration 28
Figure 5-2 3D lateral model demonstration 29
Figure 5-3 3D model demonstration 29
Figure 5-4 2D finite element model 35
Figure 5-5 3D finite element model 36
Figure 5-6 3D finite element model with torsional restraint 37
Figure 5-7 1.5D removed 50’ arm length lateral analysis 38
Figure 5-8 50’ arm length lateral reaction analysis 42
Figure 5-9 50’ arm length in cohesive soil 44
Figure 5-10 50’ arm length in cohesionless soil 45

List of Notations

D – Diameter of shaft

E – Elastic modulus

I – Moment of inertia

K_h – Coefficient of horizontal subgrade reaction

c – Undrained shear strength for undisturbed cohesive soil

γ– Effective soil weight

σ'_{vz} – Effective vertical stress of soil layer

δ – Effective soil-foundation interface friction angle.

φ – Angle of internal friction for cohesionless soil

ν – Poisson's ratio

M_F – Factored moment

M_f – Moment obtained by finite element method

Chapter 1: Introduction

1.1 Problem Statement and research motivation

In Maryland, drilled shaft is used as the foundation of mast arm traffic signal structures. The drilled shaft can be referred as a bored-cast-in-situ pile and it is one type of deep foundations which facilitate load from superstructures to transfer to deeper firm strata (Murthy 2003). The first step of drilled shaft construction is to drill a hole and remove soil and rock by a bored piling machine. After an excavated hole was formed, reinforcement of shaft body would be installed and then concrete poured in. Drilled shafts are generally utilized for bridges and large-scale structures since they may resist high vertical force, lateral force, ground moment and torsional load. The advantages of drilled shaft include economics, reducing pile cap needs and easily adaptable to varying site conditions. On the other hand, there are some disadvantages of drilled shaft including extremely sensitive to construction procedures, not good for contaminated sites, and lack of qualified inspectors (FDOT Drilled Shaft Inspector Tutorial 2015).

The mast arm signal pole structures in the State of Maryland are designed based on 1994 AASHTO. However, fatigue design was not made in the AASHTO Specifications until 2001, and thus fatigue load demand on mast arm signal support structures. To provide more strength against fatigue, the size of super-structures is required to be modified. Along with size enlargement, reactions from super-structure applying on the shaft also increase. Therefore, the capacity of shaft is supposed to be verified to meet higher requirement. Shaft embedment length is a main factor of checking to provide adequate load capacity and acceptable displacement with various soil properties. For shaft body, the reinforcement design strength should be checked for axial force and bending moment.

1.2 Research Objective

The object of this research is to verify capacity of shaft foundation connected with mast arm traffic signal structures based on the AASHTO Load and Resistance Factor Design (LRFD). Verification includes three parts: embedment length, reinforcement concrete design and torsion capacity. Furthermore, finite element models would be established as comparison with analytical methods. In the AASHTO Standard Specifications for Structural Support for Highway Luminaires, and Traffic Signals (2015), Broms method is the fundamental theory for estimating capacity of shaft foundation. Broms method provides formula to determine the embedment length and diameter of shaft with ground moment and shear force under certain soil properties. With the reactions yielded by Broms method, the reinforcement section design could be checked by the P-M interaction diagram of shaft. Final verified item is the torsional capacity which is not mentioned in the AASHTO design code. However, for signal pole structures torsion caused by wind load is the largest force effect from superstructures. Another goal of this research is to compare the results based on analytical solutions from Broms method and finite element method. If reaction result of finite element method is consistent with that based on Broms method, it means finite element model could be governed by Broms method. By validating the accuracy of finite element model, the torsion effect and various soil conditions out of the design code are also considered in the finite element model.

1.3 Thesis Organization

In chapter 2, literature review is focused on lateral force transferring through soil and torsional capacity estimating methods from previous studies and reports. Analytical methods consisting of embedment length and torsion capacity are mentioned in the chapter 3. Based on analytical methods mentioned in chapter 3, verification cases conducted with current shaft design are in chapter 4. Lateral capacity, torsional resistance and reinforcement check are verified with both cohesive and cohesionless soil. Two-dimensional and three-dimensional finite element models are built to validate lateral and torsional analyses. The results including lateral stress distribution, maximal bending moment and shear stress and torsional capacity are compared with those based on analytical methods. Conclusions and potential future work are presented in Chapter 6.

Chapter 2: Literature review

2.1 Lateral soil reaction

2.1.1 Lateral load capacity of pile foundation

Drilled shaft is a type of pile foundation employed by traffic signal mast arm structures to resist external loads. The foundation of traffic signal structures is mainly subjected to lateral force which could lead to failure in deflection. According to Broms category (1964), behaviors of shaft could be classified as long pile and short pile for free-head and fixed-head piles by dimensionless quantity βL, where

$$\beta = \left(\frac{kd}{4EI}\right)^{0.25} \tag{2-1}$$

EI= stiffness of pile section

k= coefficient of horizontal subgrade reaction

d= diameter of pile

L= length of pile

Table 2-1 Pile classification under laterally loaded (Broms 1964)

Pile type	Long Pile	Short Pile
Free-head Pile	βL > 2.5	βL < 2.5
Fixed-head Pile	βL > 1.5	βL < 1.5

Shaft foundation is usually classified as a short pile which behaves rigidly. The goals of designer are to determine deflections and stresses in the selected soil-pile system in order that they may be controlled within tolerable limits (Davisson, M. T. 1970). Failure of

laterally loaded pile occurs either when bending moment of pile reaches ultimate or lateral earth pressure reaches ultimate lateral soil resistance. The mode of failure for a short pile is like a rigid body rotating with respect to a point located near the toe of pile. Unlike short pile, the mode of failure for a long pile is a plastic hinge forming at the section of maximum bending moment.



Figure 2-1 Short pile

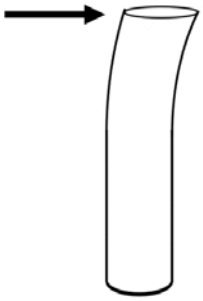


Figure 2-2 Long pile

2.1.2 Elastic analysis

The relationships between pile deflection (y) and soil reaction (p) along depth (x) could be derived by the following equations.

slope of the deflected pile $S = \frac{dy}{dx}$ (2-2a)

moment of pile $M = EI\frac{d^2y}{dx^2}$ (2-2b)

shear $V = EI\frac{d^3y}{dx^3}$ (2-2c)

soil reaction $P = EI\frac{d^4y}{dx^4}$ (2-2d)

where EI is the flexural stiffness of pile.

The soil reaction P could be assumed as $P = -E_s y$, where E_s represents the soil modulus, which may be expressed as $-\frac{P}{y}$. The deflection (y) at certain depth (x) could be solved by differential equations shown below with sufficient boundary conditions.

$$EI\frac{d^4y}{dx^4} + E_s y = 0 \tag{2-3}$$

2.1.3 Non-rigid Soil-Structure Interaction Analyses

In the 1940's and 1950's, energy companies began to install offshore foundations which had to resistant horizontal loads from waves. Therefore, foundation model was developed to simulate structural behavior under ultimate lateral force. Field tests started in the 60s and 70s, e.g. Broms (1964), Matlock (1970) and Reese and Cox (1975). Design recommendation has been established by the American Petroleum Institute (API) based on previous research studies for offshore foundation structures since 1987 (FindAPile.com).

Soil is assumed as a series of linear or non-linear springs connected with pile foundations to represent the interaction between soil and piles. Unlike rigid analyses merely viewing soil reaction as a force, the soil-structure interaction, soil's response to lateral loads and deformation of soil are considered. Those assumptions are essential to conduct numerical analyses and finite element model establishment.

Initially, soil spring is a concept proposed by Winkler which is numerical solutions of soil lateral force termed as soil modulus based on Winkler's assumption. Soils surrounded with pile foundation are approximated by a series of independent elastic springs. However, Winkler's hypothesis does not account for soil deformation and limited with surface load applied. To improving Winkler assumption, the p-y method simulates the soil resistance as

nonlinear behavior, where p is the soil pressure per unit length of the pile and y is the pile deflection. The earliest p-y analysis proposed for soil non-linear behavior could be dated back to the 1950's and this concept is developed by Skempton and Terzaghi (Ruigrok 2010).

The p-y method is applicable for numerical model by using a two-dimensional finite difference analysis. The pile foundation is divided into n intervals with nodes and soil assumed as a series of non-linear springs connected to each node. Reactions, including shear, moment and lateral deflection, could be computed with flexural stiffness for each interval and soil spring stiffness defined by p-y curve. The p-y curve could be obtained by field test and the experiment began in the late 1950s. However, the performance of those methods is limited and full-scale load test is required to calibrate those methods (Coduto 2001).

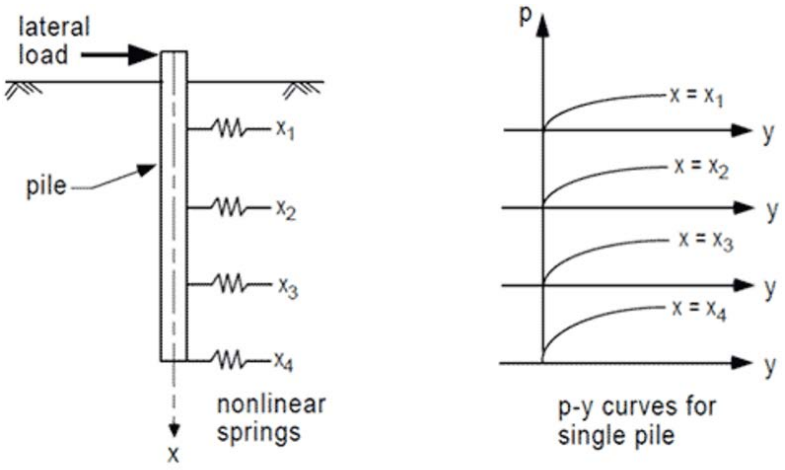


Figure 2-3 Single pile model (FHWA 2010)

2.1.4 The p-y curve classification

In American Petroleum Institute (API) design code, lateral bearing capacity and p-y curve are classified by soil properties, including soft clay stiff clay and sand. It is recommended to apply constructed stress-strain data from laboratory soil samples in the design procedure. For soft clay, unit lateral bearing capacity varies from 8 times to 12 times undrained shear strength (c) in static condition from experiments. Lateral soil resistance-deflection relationships for piles in soft clay are generally non-linear and the p-y curves for the short-term static load are provided by the following Table 2.2:

Table 2-2 p-y curve for soft clay (API 2005)

p/pu	y/yc
0.00	0.0
0.23	0.1
0.33	0.3
0.50	1.0
0.72	3.0
1.00	8.0
1.00	∞

where

c = undrained shear strength for undisturbed clay soil samples, psi (kPa),

p = actual lateral resistance, psi (kPa),

y = actual lateral deflection, in. (m),

$y_c = 2.5\ \varepsilon_c D$, in. (m),

ε_c = strain which occurs at one-half the maximum stress on laboratory unconsolidated undrained compression tests of undisturbed soil samples.

For stiff clay, unit lateral bearing capacity of soft clay varies from 8 times to 12 times undrained shear strength (c) in static condition. Compared with soft clay, stiff clays behave more brittle but are still with non-linear stress-strain relationships.

For sand, the ultimate lateral bearing capacity for sand is determined by Eq.2-4 at shallow depths. In deep depth case, lateral bearing capacity is determined by Eq.2-5.

$$p_{us} = (C1 \times H + C2 \times D) \times \gamma \times H \quad (2\text{-}4)$$

$$p_{ud} = C3 \times D \times \gamma \times H \quad (2\text{-}5)$$

where

p_u = ultimate resistance (force/unit length), lbs/in. (kN/m) (s = shallow, d = deep),

γ = effective soil weight, lb/in^3 (kN/m^3),

H = depth, in. (m),

φ' = angle of internal friction of sand, (deg).

C1, C2, C3 = Coefficients determined by function of φ',

D = average pile diameter from surface to depth, in. (m).

The lateral soil resistance-deflection (p-y) relationships for sand are also non-linear and in absence of more definitive information may be approximated at any specific depth (H), by the following expression:

$$P = A \times p_u \times \tanh\left[\frac{k \times H}{A \times p_u} \times y\right] \quad (2\text{-}6)$$

where

A = factor to account for cyclic or static loading condition.

Evaluated by:

A = 0.9 for cyclic loading.

A= $(3.0-0.8\frac{H}{D}) \geq 0.9$ for static loading.

p_u = ultimate bearing capacity at depth H, lbs/in. (kN/m),

k = initial modulus of subgrade reaction, lb/in.3 (kN/ m^3).

y = lateral deflection, inches (m).

2.2 Torsional capacity

In the AASHTO Standard Specifications for Structural Support for Highway Luminaires, and Traffic Signals (2015), torsional capacity of shaft foundation is not considered in the design procedure. However, torsional load transfer between drilled shaft and soil is relatively critical when wind load is applied.

In the analytical method, torsional capacity consists lateral resistance and bottom resistance and could be expressed as (Oregon DOT 2016)

$$T_{total} = T_s + T_b \tag{2-7}$$

where

T_{total} = total torsional resistance

T_s = lateral torsional resistance

T_b = bottom torsional resistance

The torsional resistance is caused by either cohesion of soil or friction between soil and shaft. For shaft installed in cohesive soil, the resistance is caused by cohesion of soil which is related to soil contacting area of foundation. For shaft installed in cohesionless soil, the resistance is mainly from the friction between shaft and soil caused by earth lateral force and self-weight of foundation.

2.2.1 Unit resistance of soil

The ratio between cohesion and undrained shear strength of soil was found by Tomlinson (1970) and he proposed the table below to determine the adhesion factor (α). The adhesion factor (α) is a function of undrained shear strength for the stratum of interest and proposed by O'Neill and Rees (Oregon DOT 2016). This method is widely applied to evaluate side resistance for pile axial capacity. In the Florida District 7 Method (Hu 2003) and IDOT, the alpha method is adopted to evaluate unit shaft torsional resistance.

Table 2-3 Adherence factors for pile driving in stratified soils Tomlinson (1970)

Soil conditions	Penetration ratio	α
Sands or sandy soils overlying stiff cohesive soils	<20	1.25
	<20	
Soft clays or silts overlying stiff cohesive soils	<20 (>8)	0.4
	>20	0.7
Stiff cohesive soils without overlying strata	<20 (>8)	0.4
	>20	

For cohesionless soil, the β-Method (e.g., O'Neill and Hassan, 1994) is employed to estimate unit torsional resistance for shaft under axial loading. The β-Method could be used to evaluate load capacity of piles in both cohesive and cohesionless soils (BOGUMIŁ 2015). The β-method is adopted by Florida District 5 Method and IDOT design method to estimate unit resistance. β factor is the load transfer ratio of effective soil stress and soil resistance (r_s), where

$$r_s = \beta\sigma'_{vz} \tag{2-8}$$

2.2.2 Torsion test

Mentioned in previous studies, there are three main types of torsional loading tests, including small-scale model shaft at 1g, small-scale multi-g centrifuge shafts and full-scale shafts (ODOT, 2016). Small-scale model at 1 g test (Poulos, 1975) is performed with circular aluminum piles whose sizes are around 1% of the actual shaft. Resistance strain gages re installed to measure rotational strain and obtain the relationship between applied torque and rotation in different soil. Small-scale multi-g centrifuge shafts (Bizaliele, 1992) test is conducted with 1:100 aluminum model piles at a chosen acceleration level of 50g. The applied load and result are measured by using a load cells and linear variable displacement transducers. The shaft resistance at each level could be obtained from shear strain. The result of centrifuge test was used to determine the depth of drilled shafts subjected to combined torsion and lateral load in Florida. Compared to small scale test, full scale test of drilled shaft is rare. The latest full-scale test (McVay et al. 2014) is conducted with three drilled shafts whose diameter range is from 4 feet to 12 feet and embedment length range is from 12 to 18 feet, and all shaft heads are 1.5 feet above ground surface. Unlike small model test, result of full scale test provides torsional resistance along the depth with various soil layers.



Figure 2-4 Combined torsion and lateral loading (McVay et al. 2014)

Chapter 3: Analytical verification

3.1 Embedment length

For cohesive soil, the shaft embedment length (L) is determined by shaft diameter (D), ultimate shear strength of soil, moment, and shear at groundline. The required embedment length (L) by AASHTO LTS-1 to 6 and LRFDLTS-1 Specifications (2015) can be found：

$$L = 1.5D + q[\,1 + \sqrt{2 + \frac{(4H+6D)}{q}}\,] \qquad \text{(AASHTO C13.6.1.1-1)}$$

where:

$$H = \frac{M_F}{V_F} \qquad \text{(AASHTO C13.6.1.1-2)}$$

$$q = \frac{V_F}{9cD} \qquad \text{(AASHTO C13.6.1.1-3)}$$

M_F= Factored moment at groundline (kip-ft)

V_F= Factored shear at groundline (kip)

D = Diameter of shaft (ft)

c = the ultimate shear strength of cohesive soil (ksf)

$$M_u = V_F(H + 1.5D + 0.5q) \qquad \text{(AASHTO C13.6.1.1-4)}$$

Maximal moment (M_u) is located at $(1.5D + q)$ below groundline.

For cohesionless soil, shaft embedment length is determined by shaft diameter, angle of internal friction, effective unit weight, moment, and shear at groundline. Required embedment length L by AASHTO LTS-1 to 6 and LRFDLTS-1 Specifications (2015) can be found by using trial and error equation shown below:

$$L^3 - \frac{2V_F L}{K_p \gamma D} - \frac{2M_F}{K_p \gamma D} = 0 \qquad \text{(AASHTO C13.6.1.1-5)}$$

Where:

$$K_p = \tan^2(45 + \frac{\varphi}{2}) \qquad \text{(AASHTO C13.6.1.1-6)}$$

γ = unit weight of cohesionless soil (kcf)

For the required embedment length (L), the maximum moment in the shaft can be calculated as:

$$M_u = V_F(H + 0.54\sqrt{\frac{V_F}{\gamma D K_p}}) \qquad \text{(AASHTO C13.6.1.1-1)}$$

And located at $0.82\sqrt{\frac{V_F}{\gamma D K_p}}$ below groundline.

3.2 Torsional Capacity

In addition to loading test, there are four analytical methods for torsional capacity. Generally, the torsional capacity of drilled shafts (T_{total}) consists lateral (T_s) and bottom (T_b) torsional resistance.

$$T_{total} = T_s + T_b \qquad (3\text{-}1)$$

The first method is the Florida Structure Design office method which assumes that the soil behaves as a rigid, perfectly-plastic material and the shaft behaves as a rigid body under simple torsional load at the ultimate or fully-mobilized soil resistance. Unit shaft resistance r_s in cohesionless soil

$$r_s = K_0 \sigma'_{vz} tan\delta \quad (3\text{-}2)$$

Where

K_0 = at rest lateral earth pressure coefficient

σ'_{vz}= effective vertical stress at the midpoint of the layer of interest

δ = effective soil-shaft interface friction angle

Then, the total shaft resistance can be obtained by:

$$T_s = \frac{\pi D^2}{2} L r_s \quad (3\text{-}3)$$

where

D = shaft diameter,

L = shaft length.

The toe resistance may be estimated using:

$$T_b = \frac{D}{3} W tan\delta \quad (3\text{-}4)$$

where

W = shaft weight. the axial load applied on drilled shafts is neglected for evaluating the toe resistance using this method.

The second method is the Florida District 5 Method. The ultimate shaft resistance, Q_s is obtained from SHAFTUF program.

$$T_s = \frac{D}{2} Q_s \quad (3\text{-}5)$$

$$T_b = \frac{D}{3} (W + Q_a) \tan\left(\frac{2}{3}\delta\right) \quad (3\text{-}6)$$

where

Q_a = axial load applied on drilled shafts, and all the other variables have been defined previously.

The second approach employs the β-Method (e.g., O'Neill and Hassan, 1994) for shafts under axial loading. In this approach, the unit shaft resistance in cohesionless soil is given by:

$$r_s = \beta\sigma'_{vz} \tag{3-7}$$

where

β = load transfer ratio for effective-stress normalized unit shaft resistance and has been correlated to depth and the STP blow count, N:

$$\beta_{nominal} = 1.5 - 0.135\sqrt{z}, 1.2 \geq \beta_{nominal} \geq 0.25 \text{ for } N \geq 15$$

$$\beta = \frac{N}{15}\beta_{nominal} \text{ for } N < 15$$

where

z = depth from ground surface to the mid-layer of interest.

Then, the total shaft resistance can be obtained using Equation (3-4). The toe resistance is estimated using:

$$T_b = \frac{D}{3}(W + Q_a)\tan\delta \tag{3-8}$$

The third method is the Florida District 7 Method. Unit shaft resistance r_s in cohesionless soil:

$$r_s = \alpha S_u + K_0\sigma'_{vz}tan\delta \tag{3-9}$$

Where

S_u = average undrained shear strength over the depth of interest

K= coefficient of lateral earth pressure ranging from K_0 to 1.75

α= an adhesion factor, which is a function of the average undrained shear strength for the stratum of interest, as proposed by O'Neill and Reese (O'Neill and Reese 1999) for shafts under axial loading:

$$\alpha = 0.55 \text{ for } \frac{S_u}{P_a} \leq 1.5$$

$$\alpha = 0.55 - 0.1\left(\frac{S_u}{P_a} - 1.5\right) \text{ for } 1.5 \leq \frac{S_u}{P_a} \leq 2.5$$

$$\alpha = 0.45 \text{ for } \frac{S_u}{P_a} \geq 2.5$$

where

Pa = atmospheric pressure in the same units as S_u. It is suggested that when S_u/P_a is larger than 2.5, the shaft resistance under axial loading should be calculated by considering the cohesive soil as intermediate geometrical (O'Neill and Reese 1999).

The unit soil N ≥15resistance from ground surface to a depth of 1.5 m or to the depth of seasonal moisture change is neglected due to the potential loss of shaft resistance as soil expands and contracts induced by wetting and drying or freezing and thawing near the ground surface (Brown et al. 2010).

The torsional shaft resistance, T_s, is given by:

$$T_s = \frac{\pi D^2}{2}(L - 1.5)r_s \quad (3\text{-}10)$$

T_b, is estimated by

$$T_b = \frac{4\mathrm{D}}{9}(W + Q_a)tan\delta \tag{3-11}$$

The last method is the CDOT Design Method. In the CDOT Design Method, the unit shaft resistance in cohesive soils is equal to the undrained shear strength over the depth of interest, and the side resistance in cohesive soils for the top 1.5D of the shaft is neglected. The shaft resistance, T_s, for cohesive soils is given by:

$$T_s = \frac{\pi D^2}{2}(L - 1.5D)S_u \tag{3-12}$$

The toe resistance, T_t, is given by:

$$T_b = \frac{\pi D^3}{12}S_u \tag{3-13}$$

For shafts in cohesionless soils, the unit shaft resistance is given by:

$$r_s = K_0\sigma'_{vz}tan\delta \tag{3-14}$$

where

K = the coefficient of lateral earth pressure is given by:

$$\mathrm{K} = \frac{2L}{3D}(1 - \sin\emptyset') \tag{3-15}$$

Chapter 4: Analytical verification for general soil in Maryland

4.1 Embedment length check

In the embedment length check, soil conditions are assumed as general properties in Maryland shown in Table 4-1.

Table 4-1 Assumed properties of soil for hypothetical cases

Soil Type	Soil Category	Shear Strength (ksf)	Unit Weight (kcf)	Internal Friction Angle
Cohesive	Stiff clay	2.16	N/A	N/A
Cohesionless	Clean gravel-sand	N/A	0.12	30

The external loads including ground and moment are obtained by LRFD Strength I shown in Table 4-2. Both of shear force and moment are the root mean square of combined loads in the x and z directions and the load factor is 1.6.

Table 4-2 Ground shear and moment (LRFD Strength I)

Arm length (ft)	Factored Ground shear (kips)	Factored Ground Moment (kip-ft)
50	4.75	125.50
60	4.64	138.30
70	5.24	167.43
75	5.35	174.70

Based on the Broms' method used in the AASHTO LRFD Standard Specifications for Structural Support for Highway Luminaires, and Traffic Signals, the required embedment length for each mast arm with assumed soil properties are listed in Table 4-3.

Table 4-3 Embedment length verification

Arm Length	Soil Type	Required length (ft)	Design Length (ft)	Length Check
50 ft	Cohesive	7.76	10	OK
	Cohesionless	8.92	10	OK
60 ft	Cohesive	8.98	10	OK
	Cohesionless	8.24	10	OK
70 ft	Cohesive	9.27	10	OK
	Cohesionless	8.78	10	OK
75 ft	Cohesive	9.33	10	OK
	Cohesionless	8.89	10	OK

4.2 Reinforcement concrete design check

In the Broms' method, the maximal reaction moment and its location on the shaft foundation could be estimated. Therefore, reinforced concrete design could be verified by the interaction diagram. Rebars of shaft are distributed circularly and its number and size are shown in the Table 4-4.

Table 4-4 Standards for highways and incidental structures

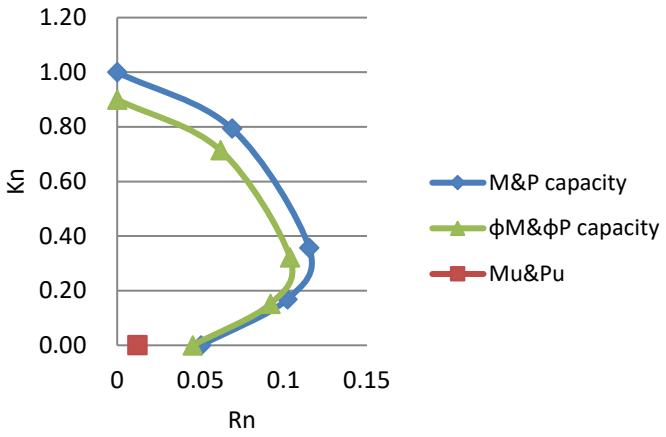
MAST ARM ARM LENGTH OR POLE SIZE	BOLT CIRCLE (IN.)	ANCHOR BOLT SIZE (IN. x IN.)	ANCHOR BOLT MAX. PROJECTION ABOVE FOUNDATION (IN.)	FOUNDATION REINFORCEMENT				CONCRETE REQUIRED
				DIAMETER (FT.)	HEIGHT (FT.)	VERTICAL REINF.	HORIZONTAL REINF.	
38' SINGLE	16	$1\,{}^{1}/_{2} \times 54$	$6\,{}^{1}/_{2}$	3	10	8 NO. 10	NO. 4 @ 12" C.C.	2.7
50' SINGLE AND TWIN	18	$1\,{}^{3}/_{4} \times 66$	$7\,{}^{1}/_{2}$	3	10	8 NO. 10	NO. 4 @ 12" C.C.	2.7
60' & 70' SINGLE	22	2×72	8	4	10	16 NO. 10	NO. 4 @ 12" C.C.	4.7
50'/60'-75'	22	2×72	8	4	10	16 NO. 10	NO. 4 @ 12" C.C.	4.7

The moment and axial load capacity of reinforced concrete could be plotted as an interaction diagram. There are five critical stages including “axial load only”, “zero tension in rebar”, “balanced condition”, “tension controlled” and “flexure only” to form the interaction diagram of reinforcement concrete column capacity. In order to make interaction diagram dimensionless, the load and moment could be transferred as following equations

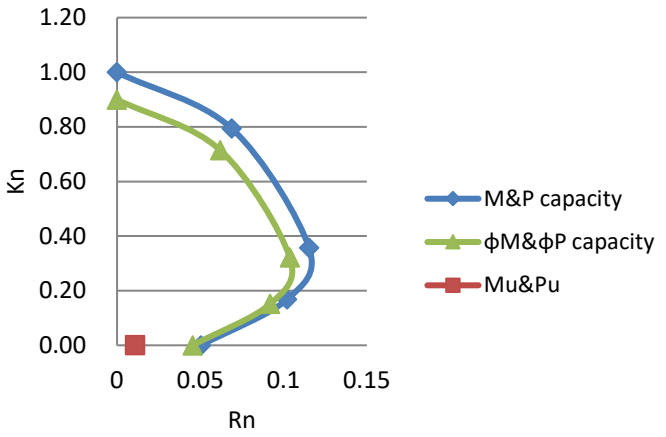
$$K_n = \frac{P_n}{f_c{}' A_g} \tag{4-1}$$

$$R_n = \frac{M_n}{f_c{}' A_g h} \tag{4-2}$$

The y-axes K_n represents axial load (P) and x-axes R_n represents moment (M) in dimensionless. In the P-M interaction, both of ultimate moment and axial load are supposed within interaction curve which means the capacity of reinforcement design of shaft is sufficient to resist extremely external loads rather than concrete cracking. The interaction diagrams of 50’, 60’. 70’ and 75’ arm lengths reinforcement concrete design in either cohesive or cohesionless soils are listed in the following figures.

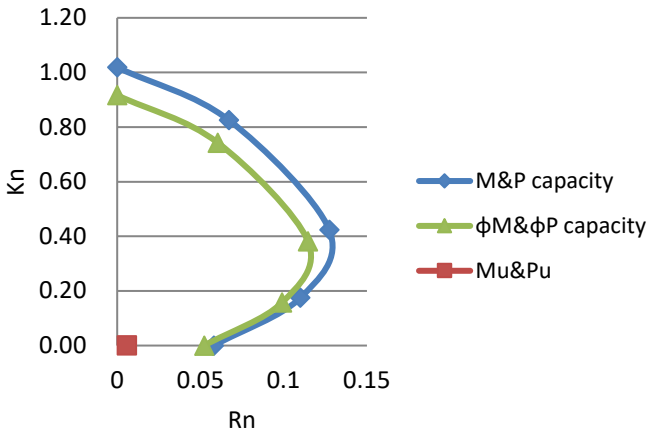


(a) Shaft in cohesive soil

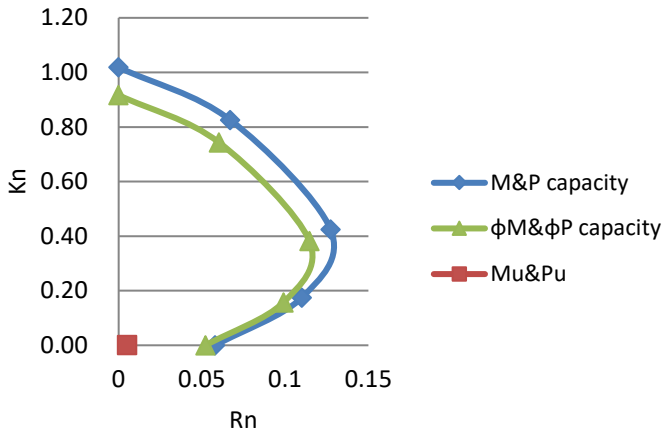


(b) Shaft in cohesionless soil

Figure 4-1 P-M interaction curve for 50' arm length signal structure

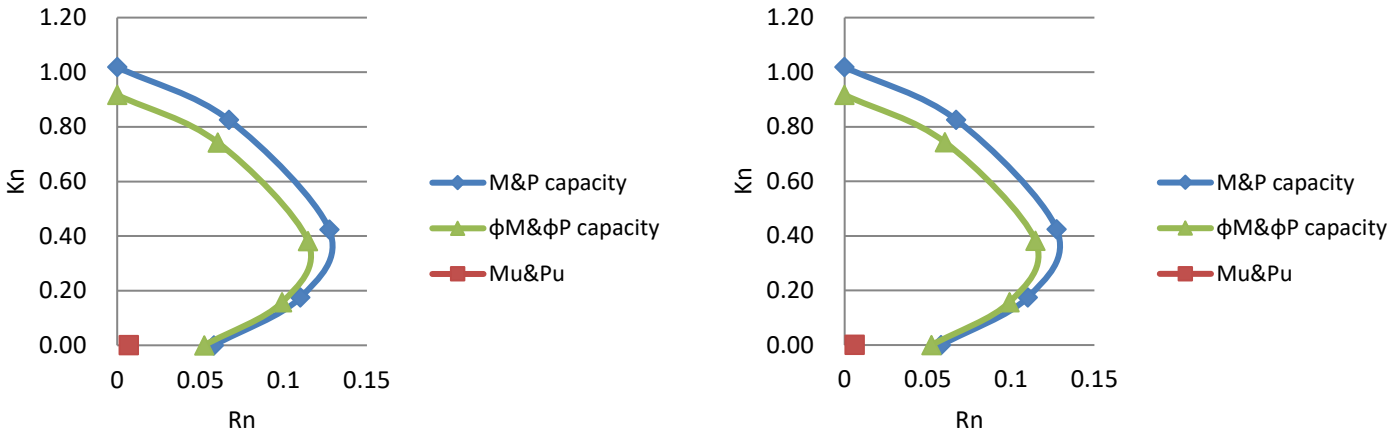


(a) Shaft in cohesive soil



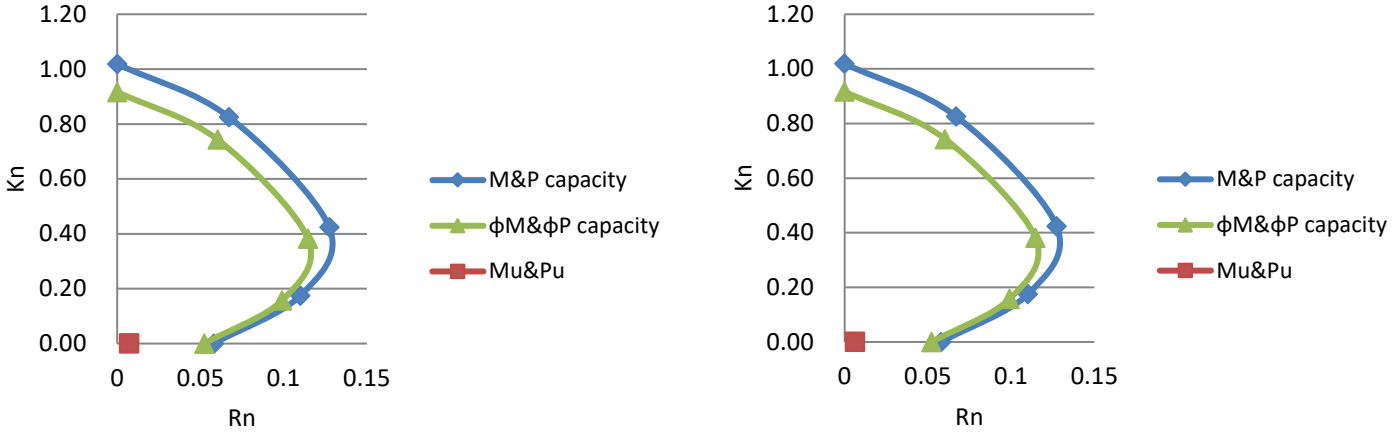
(b) Shaft in cohesionless soil

Figure 4-2 P-M interaction curve for 60' arm length signal structure



(a) Shaft in cohesive soil (b) Shaft in cohesionless soil

Figure 4-3 P-M interaction curve for 70' arm length signal structure



(a) Shaft in cohesive soil (b) Shaft in cohesionless soil

Figure 4-4 P-M interaction curve for 75' arm length signal structure

4.3 Torsional capacity check

Torsional capacity is rarely mentioned in AASHTO Standard Specifications for Structural Support for Highway Luminaires, and Traffic Signals. The evaluation methods used in Florida, Colorado and Illinois are collected and compared in this section. Two shaft sizes are considered in the torsional capacity evaluation based on soil properties assumed in

previous sections. In cohesive soil, the torsional capacity estimated by all of four methods is sufficient enough to resist horizontally rotation caused by LRFD Strength I load combination in worst condition. In cohesionless soil, most of torsional capacity is insufficient when external load reaches the peak value.

Table 4-5 3'X10' shaft torsional capacity

Cohesive				
Method	Lateral (kip-ft)	Bottom (kip-ft)	Total Capacity (kip-ft)	Maximal Applied Torque (kip-ft)
FD7	163.57	8.16	171.73	83.02
CDOT	167.95	15.26	183.22	83.02
IDOT	197.95	N/A	167.95	83.02
Cohesionless				
Method	Lateral (kip-ft)	Bottom (kip-ft)	Total Capacity (kip-ft)	Maximal Applied Torque (kip-ft)
FSDOM	24.48	6.12	30.06	83.02
FD7	20.81	8.16	28.97	83.02
CDOT	54.41	8.47	62.89	83.02
IDOT	91.02	N/A	91.02	83.02

Table 4-6 4'X10' shaft torsional capacity

Cohesive				
Method	Lateral (kip-ft)	Bottom (kip-ft)	Total Capacity (kip-ft)	Maximal Applied Torque (kip-ft)
FD7	290.80	19.34	310.14	131.81
CDOT	214.14	36.19	253.33	131.81
IDOT	298.57	N/A	298.57	131.81
Cohesionless				
Method	Lateral (kip-ft)	Bottom (kip-ft)	Total Capacity (kip-ft)	Maximal Applied Torque (kip-ft)
FSDOM	43.53	14.51	58.04	131.81
FD7	37.00	19.34	56.34	131.81
CDOT	72.55	17.65	90.20	131.81
IDOT	161.81	N/A	161.81	131.81

Chapter 5: Finite element modeling

5.1 Finite element model design

5.1.1 Model dimension and soil properties

The shaft foundation dimension and soil properties are given in below table

Table 5-1 Finite element model parameter

Diameter (D)	Embedment length (L)	Elastic modulus (E_c)	Poisson's ratio (v)
3 ft	10	519119	0.3
4 ft	10	519119	0.3

Table 5-2 Assumed cohesive soil properties

ultimate shear strength	Poisson's ratio (v)
2.16 (psf)	0.4-0.5

Table 5-3 Assumed cohesionless soil properties

internal friction angle	effective unit weight:	Poisson's ratio (v):
30□	0.12 (k/ft^3)	0.2-0.5

5.1.2 Model design

Two-dimensional model:

Two-dimensional model is designed for Broms' simplified analysis mentioned in AASHTO. The model is built on XY plane and the external force including shear force and moment at groundline. The soil spring is assumed homogeneous and located at the other side of shear force. The passive earth pressure is neglected in this analysis.

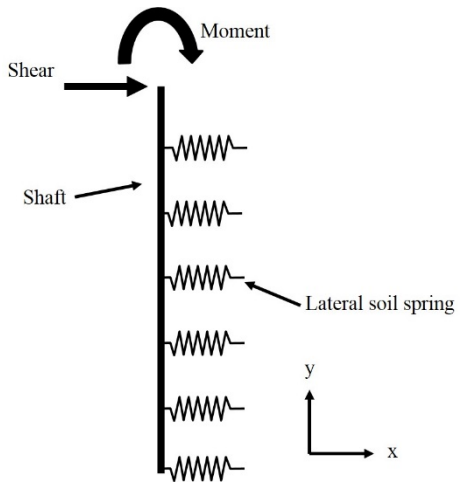


Figure 5-1 2D model demonstration

Three-dimensional model with 2D analysis:

Three-dimensional model is designed for Broms' simplified analysis mentioned in AASHTO. The model is built on XY plane and the lateral soil springs are located at x-axis and z-axis. The shear force at groundline is along x direction and the moment is about z-axis. The soil spring is assumed homogeneous and located at the other side of shear force. The passive earth pressure is neglected in this analysis.

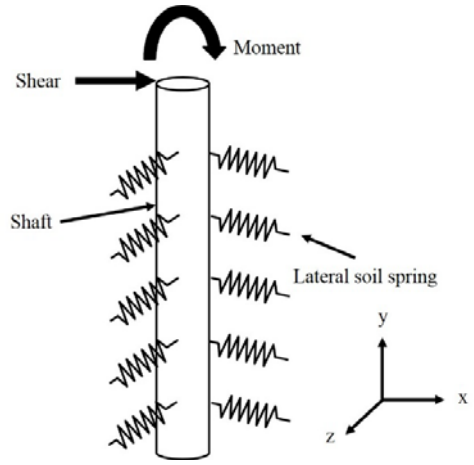


Figure 5-2 3D lateral model demonstration

Three-dimensional model:

Three-dimensional model is designed for all external forces including three translational forces, moments about z and x axes and torsion. The lateral soil springs are located at x-axis and z-axis and the torsional soil spring is located at the nodes on shaft body to restrain horizontal rotation degree of freedom. The soil spring is assumed homogeneous and located at the other side of shear force. The passive earth pressure is neglected in this analysis.

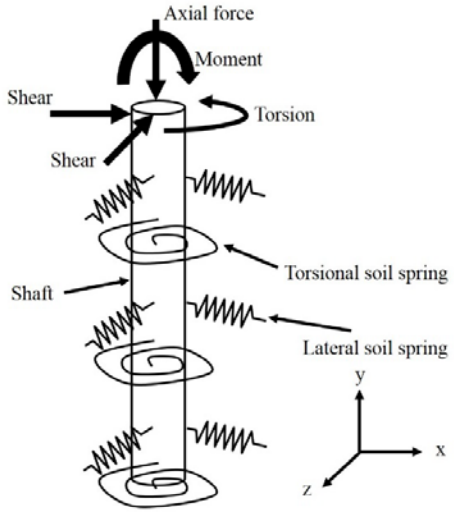


Figure 5-3 3D model demonstration

5.1.3 Soil spring

The method to estimate soil subgrade modulus is first proposed by Terzaghi (1955). Modulus of subgrade reaction of soil could be transformed into stiffness of soil spring. The soil spring stiffness represents the relationship between soil deformation and reaction. The stiffness of soil spring could be obtained from p-y curve. The soil springs include lateral, vertical, and torsional forms. Rigid analyses are used for light weight and short pile loaded laterally such as highway sign (Coduto 2001). Since shaft is defined as short pile and external loading is static and specified, the soil spring is considered under linear range. Based on soil properties mentioned before, lateral and vertical soil springs could be obtained from the table below (Fu 2014)

Table 5-4 Parameters for soil spring

	Lateral springs		Vertical springs	
Soil type	P_u	k_h	$q_{max}(ksf)$	k_q
Clay	$9c_uB$	$67c_u$	$9c_u$	$8N_{corr}$
Sand	$3\gamma Bk_px$	n_hx	$10q_{max}/z_c$	$10q_{max}/z_c$

5.1.3.1 Lateral soil spring

For cohesive soil, the stiffness of soil spring is associated with undrained shear strength and defined as below. In this research, the soil properties are assumed homogeneous; therefore, the stiffness of lateral cohesive soil spring stays constant along depth. For cohesionless soil, the stiffness of soil spring is a function of depth defined as below. Thus, the stiffness distribution is triangular.

$$p = k_h y \quad (5\text{-}1)$$

Where:

p = soil reaction per unit length of pile

y = pile deflection

k_h= subgrade reaction in units of force/length^2

Cohesive soil:

$$k_h = 67C_u \quad (5\text{-}1a)$$

Cohesionless soil:

$$k_h = n_h x \quad (5\text{-}1b)$$

Where:

$C_u = Undrained\ shear\ strength$;

$n_h = constant\ of\ subgrade\ reaction = \frac{Jr}{1.35}$;

X=depth from soil surface;

J=constant, 200 for loose sand, 600 for medium sand, 1500 for dense sand;

r= effective unit weight of soil;

5.1.3.2 Vertical soil spring

Vertical soil spring is designed for controlling shaft's vertical displacement under acceptable range. The vertical soil spring is defined as a point spring which is either associated with undrained shear strength for cohesive soil or average standard penetration blow count. The vertical spring stiffness is defined as below.

$$k_q = \frac{10q_{max}}{Z_c} \tag{5-2}$$

For cohesive soil:

$$q_{max} = 9C_u \tag{5-2a}$$

For cohesionless soil:

$$q_{max} = 8N_{corr} \tag{5-2b}$$

$$N_{corr} = N \; if \; N \leq 15$$

$$N_{corr} = 15 + 0.5(N - 15) if \; N > 15$$

5.1.3.3Torsional soil spring

Torsional spring is currently used in pile foundation analysis program such as FB-MultiPier (2011). The torsion-angle (T-θ) curve is assumed as a hyperbolic curve below.

$$\mathrm{T} = \frac{\theta}{a + b\vartheta} \tag{5-3}$$

The stiffness of torsional spring is equal to the slope of torsion-theta curve at certain theta, where

$$k_t = \frac{dT}{d\theta} \tag{5-4}$$

The torque per length of rigid pile is expressed by (Randolph 1981)

$$\frac{\Delta T}{\Delta L} = 4\pi G * r^2 \tag{5-5}$$

Therefore, the initial stiffness of torsion spring is given by

$$(\frac{dT}{d\theta})_i = \frac{1}{a} = 4\pi G * r^2 * \Delta L \tag{5-6}$$

Shear modulus (G) for cohesive soil

$$G = \frac{\beta * C_u}{2(1+\nu)} \quad (5\text{-}7)$$

Shear modulus (G) for cohesionless soil

$$G = \frac{k * z}{2(1+\nu)} \quad (5\text{-}8)$$

Soil Spring Table

Table 5-5 Cohesionless soil spring

Depth (ft)	Lateral (klf)	Vertical k (klf)	Torsional k (kip-ft)
0	0	N/A	0
1	8.89	N/A	85.92
2	17.78	N/A	343.69
3	26.67	N/A	773.31
4	35.56	N/A	1374.78
5	48.89	N/A	2148.10
6	53.33	N/A	3093.26
7	62.22	N/A	4210.27
8	71.11	N/A	5499.13
9	80.00	N/A	6959.83
10	88.89	43.74	8592.39

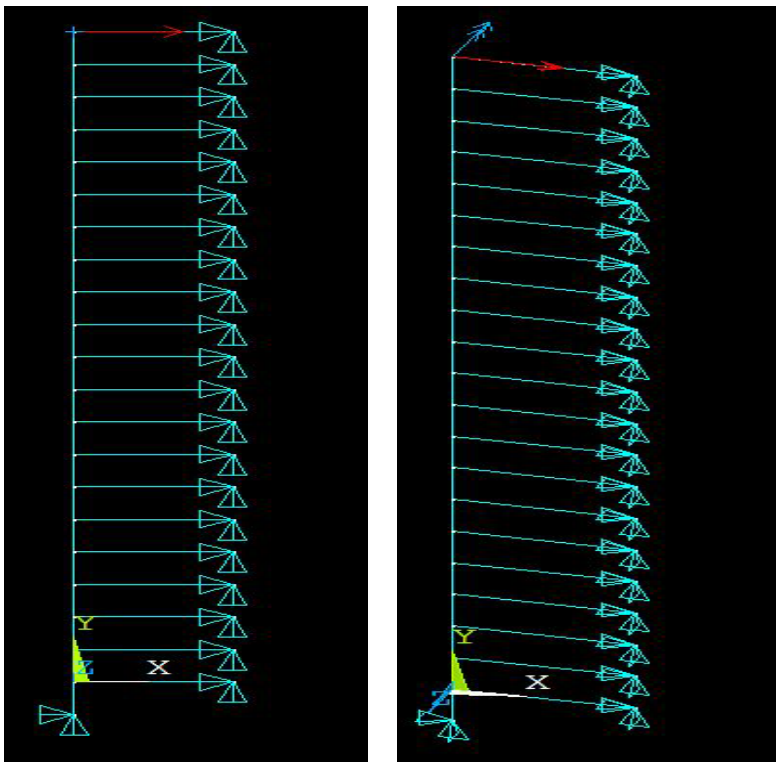
Table 5-6 Cohesive soil spring

Lateral (klf)	Vertical k (klf)	Torsional k (kip-ft)
72.36	116328	5816.43

5.2 Finite element model establishment

5.2.1 Two-dimension model

Beam 3 is adopted as the shaft body which is a uniaxial element with tension, compression, and bending capabilities. This element has three degrees of freedom at each node: translations in the nodal x and y directions and a rotation spring about the nodal z-axis. Combin14 is used to simulated soil connected with shaft which has longitudinal or torsional capabilities in one, two, or three-dimensional applications. The longitudinal spring is a uniaxial tension compression element with three degrees of freedom at each node: translations in the nodal x, y, and z directions bending and torsion are not considered. The torsional spring is a purely rotational element with three degrees of freedom at each node: rotations about the nodal x, y, and z axes. The increment of shaft body is 0.5 ft along depth. The cross area of and moment inertia are supposed to defined as constant and inputted into program. The bottom of shaft is connected with vertical soil spring and the lateral soil springs are connected along x direction. All degrees of freedom at the end of springs are fixed



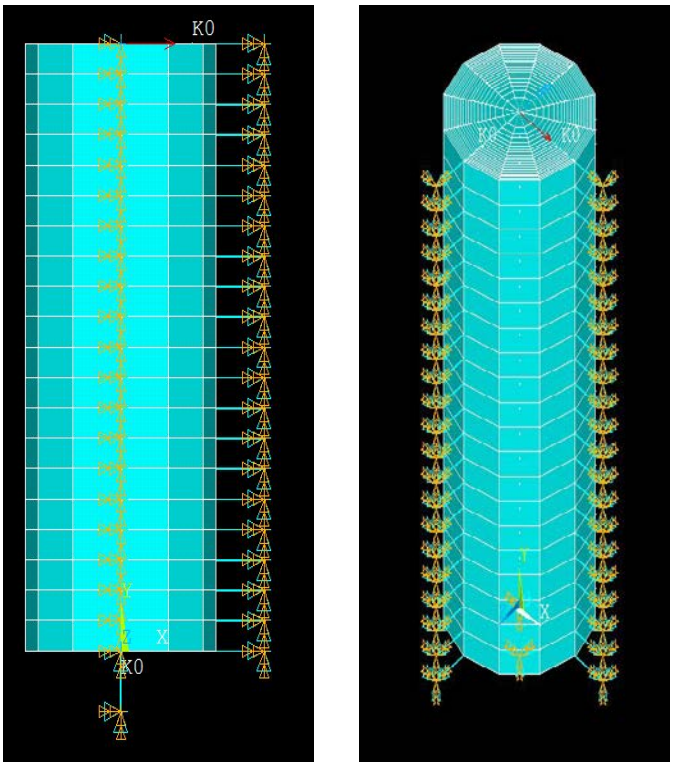
(a) Model in XY plane **(b) Model in 3-dimension**

Figure 5-4 2D finite element model

5.2.2 Three-dimensional model with 2D analysis

The BEAM188 element is used to simulate a shaft which is suitable for analyzing slender to moderately thick beam structures. This element is based on Timoshenko beam theory and shear deformation effects are included. This linear beam element is three dimensional with six degrees of freedom at each node. The degrees of freedom at each node consist of translations in x, y, and z directions, and rotations about the x, y, and z directions. BEAM188 element is suggested for linear, large rotation, and large strain nonlinear applications. Combin14 is used to simulated soil connected with a shaft which is defined as sore degree of freedom by keyopt function with real constant. The bottom of shaft is

connected with vertical soil spring and the lateral soil springs are connected along x and z directions. All degree of freedom at the end of springs are fixed.

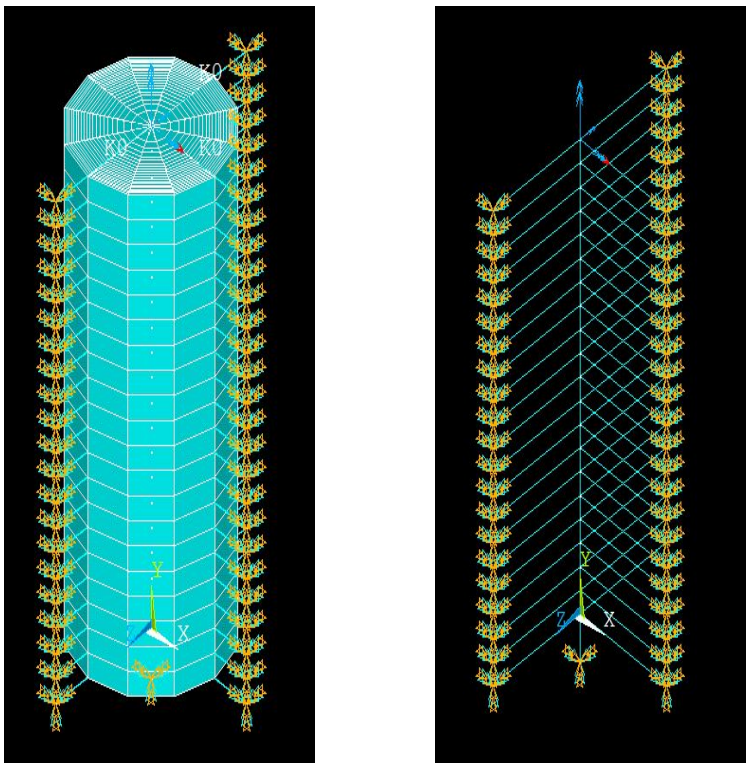


(a) Model in XY plane (b) Model in 3-dimension

Figure 5-5 3D finite element model

5.2.3 Three-dimensional model

The BEAM188 element is used for three-dimensional analysis. Since external force includes translation along x, y and z axes and rotation about x, y and z axes, the corresponding degrees of freedom should be well defined. More than 3D model with 2D analysis, the rotational degree about y axis is restrained by soil torsional spring. The torsional springs are built with additional nodes at the -z direction and connected with shaft like lateral springs. The torsional springs are also adopted Combin14 element which is defined with ROTY stiffness. All degrees of freedom at the end of springs are fixed.



(a) Model in 3-dimension **(b) Simplified 3D model**

Figure 5-6 3D finite element model with torsional restraint

5.3 Finite element method analysis result

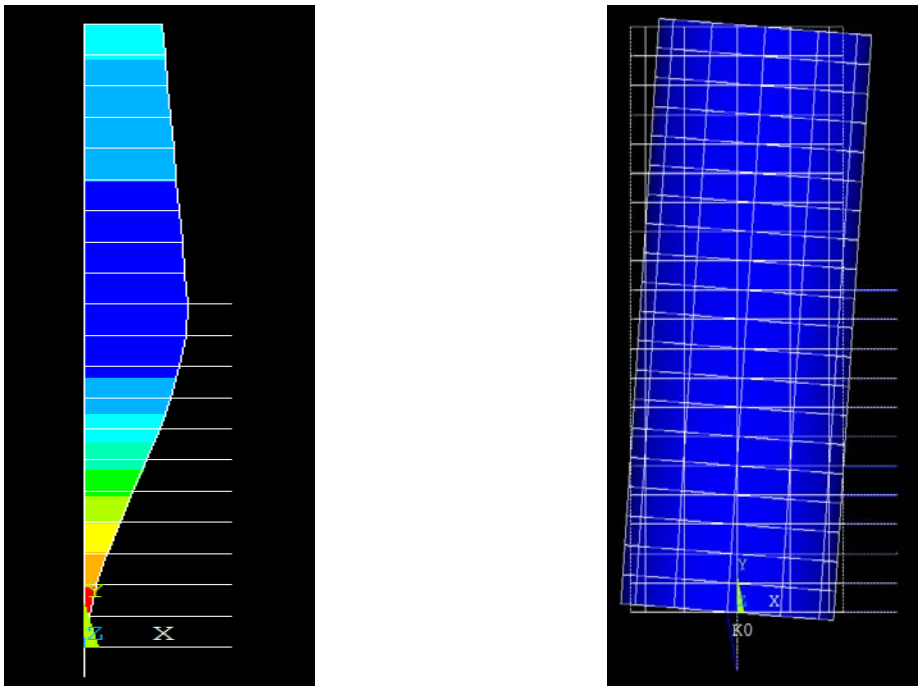
5.3.1 Cohesive soil lateral analysis

Based on Broms' assumption (1964), the model is assumed as short free head pile and the lateral soil reaction is neglected from ground surface to 1.5 shaft diameter (D) depth. However, to compare the impact caused by partially removed lateral soil reaction, three finite element models were built: 1.5D removed, 0.75D removed and non-removed. For lateral reaction analysis, 1.5D removed, 0.75D removed non-removed cohesive models are built in two-dimension and three-dimension. 1.5D removed and 0.75D removed cohesive model are built for three-dimensional analysis. Finite element models are listed in the Table 5-7. The

degrees of freedoms in the neglected zone would be released. Maximal moments (M_f) and its locations (L_f) obtained from ANSY APDL are listed and compared with moments (M_u) and locations (L) yielded from Broms' method in the following table.

Table 5-7 Finite element model list

Arm length size			
Model type	1.5 D removed	0.75 D removed	Non-removed
2D	50'-60'-70'-75'	50'-60'-70'-75'	50'-60'-70'-75'
3D	50'-60'-70'-75'	50'-60'-70'-75'	50'-60'-70'-75'



(a) 2D moment distribution **(b) 3D displacement**

Figure 5-7 1.5D removed 50' arm length lateral analysis

Table 5-8 FEM analysis result of lateral reaction 1.5D removed (cohesive)

2D model					
Length (ft)	M_u (kip-ft)	L (ft)	M_f (kip-ft)	L_f (ft)	Diff (%)
50	147.07	4.58	168.46	4.5	12.70
60	166.28	6.06	193.92	6	14.25
70	199.06	6.06	230.28	6	13.56
75	206.98	6.07	238.89	6	13.36
3D model					
Length (ft)	M_u (kip-ft)	L (ft)	M_f (kip-ft)	L_f (ft)	Diff (%)
50	147.07	4.58	166.69	4.5	11.77
60	166.28	6.06	180.12	6	7.68
70	199.06	6.06	227.69	6	12.57
75	206.98	6.07	236.22	6	12.38

Table 5-9 FEM analysis result of lateral reaction 0.75D removed (cohesive)

2D model					
Length (ft)	M_u (kip-ft)	L (ft)	M_f (kip-ft)	L_f (ft)	Diff (%)
50	147.07	4.58	149.56	2	1.66
60	166.28	6.06	166.14	3	-0.08
70	199.06	6.06	198.87	3	-0.09
75	206.98	6.07	206.80	3	-0.08
3D model					
Length (ft)	M_u (kip-ft)	L (ft)	M_f (kip-ft)	L_f (ft)	Diff (%)
50	147.07	4.58	149.43	2	1.57
60	166.28	6.06	165.82	3	-0.27
70	199.06	6.06	198.37	3	-0.34
75	206.98	6.07	206.24	3	-0.35

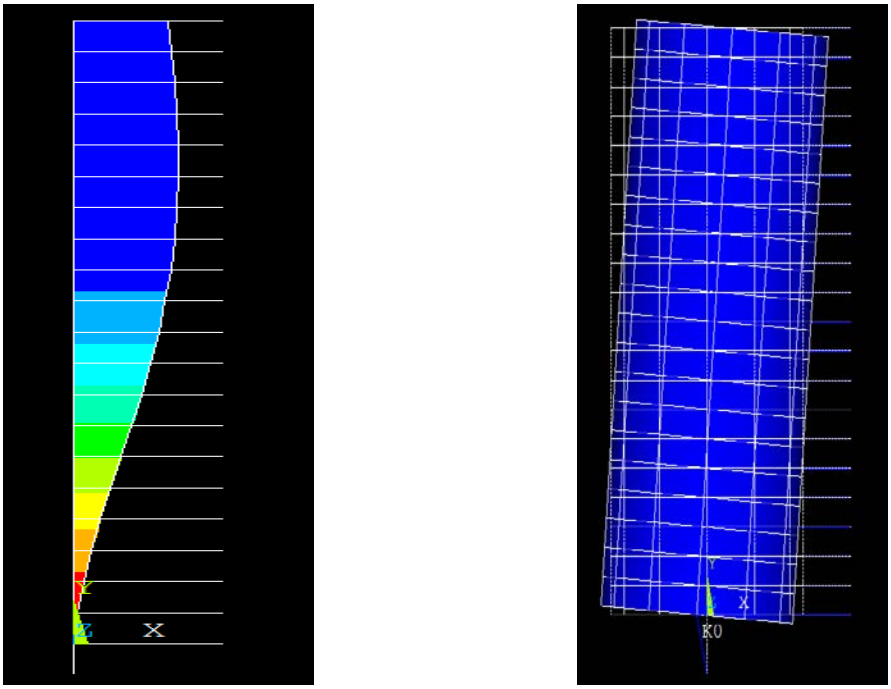
Table 5-10 FEM analysis result of lateral reaction non-removed (cohesive)

2D Model					
Length (ft)	M_u (kip-ft)	L (ft)	M_f (kip-ft)	L_f (ft)	Diff (%)
50	147.07	4.58	127.68	1	-15.19
60	166.28	6.06	140.28	1	-18.53
70	199.06	6.06	169.52	1	-17.43
75	206.98	6.07	176.79	1	-17.08
3D Model					
Length (ft)	M_u (kip-ft)	L(ft)	M_f (kip-ft)	L_f (ft)	Diff (%)
50	147.07	4.58	127.78	1	-15.10
60	166.28	6.06	140.13	1	-18.66
70	199.06	6.06	169.21	1	-17.64
75	206.98	6.07	176.43	1	-17.32

The maximum moment (M_f) obtained from 0.75D removed model is the closest to that from Broms' analytical method but the location (L_f) of maximal moment occurred is off. The maximum moment (M_f) obtained from 1.5D has about 15% difference between Broms' analytical method's outcome. Both of location (L_f) and maximum moment (M_f) yielded from Non-removed are further away from those from Broms' analytical method.

5.3.2 Cohesionless soil lateral analysis

For the cohesionless soil, the lateral soil reaction distributed triangularly and the shaft model is assumed with free end rotation. Thus, the bottom of shaft body is translation restrained in the y-direction. Shaft models are built for 50',60', 70' and 75' arm length signal structure in two-dimension and three-dimension. Maximal moment (M_f) and its location (L_f) obtained from ANSY APDL are listed and compared with maximum moment (M_u) and location (L) yielded from Broms method in the following table.



(a).2D moment distribution (b) 3D displacement

Figure 5-8 50' arm length lateral reaction analysis

Table 5-11 FEM analysis result of lateral reaction (cohesionless)

2D Model					
Length (ft)	M_u (kip-ft)	L (ft)	M_f (kip-ft)	L_f (ft)	Diff (%)
50	133.62	2.59	139.92	2.5	4.50
60	145.09	2.22	151.78	2	4.40
70	175.58	2.22	182.38	2	3.78
75	183.11	2.22	189.87	2	3.56
3D Model					
Length (ft)	M_u (kip-ft)	L (ft)	M_f (kip-ft)	L_f (ft)	Diff (%)
50	133.62	2.59	139.89	2.5	4.48
60	145.09	2.22	151.81	2	4.42
70	175.58	2.22	182.29	2	3.68
75	183.11	2.22	189.75	2	3.49

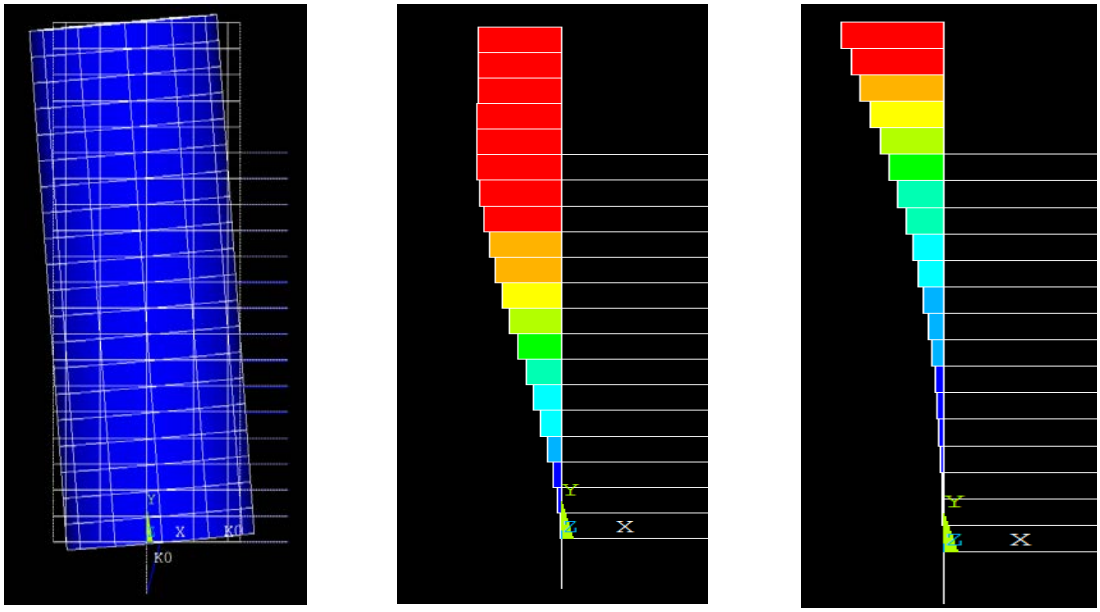
The maximum moment (M_f) and its location (L_f) yielded from finite element analysis are close to those from Broms' analytical method. The maximum moment (M_f) has less than 5% difference between M_u and the moment distributions are similar among 2D and 3D models.

5.3.3 Three-dimensional analysis in cohesive and cohesionless soil

Shaft models are built in cohesive and cohesionless soil for three-dimensional analysis and the finite element models are listed in the Table 5-12. For cohesive soil case, 1.5D and 0.75D removed models are built and compared. Ground shear, axial load, moment and torsion induced by superstructures are assigned independently along Cartesian coordinate. The shear force in the z-direction and moment about x axis are factored 1.6 in analysis procedure based on LRFD Strength I load combination.

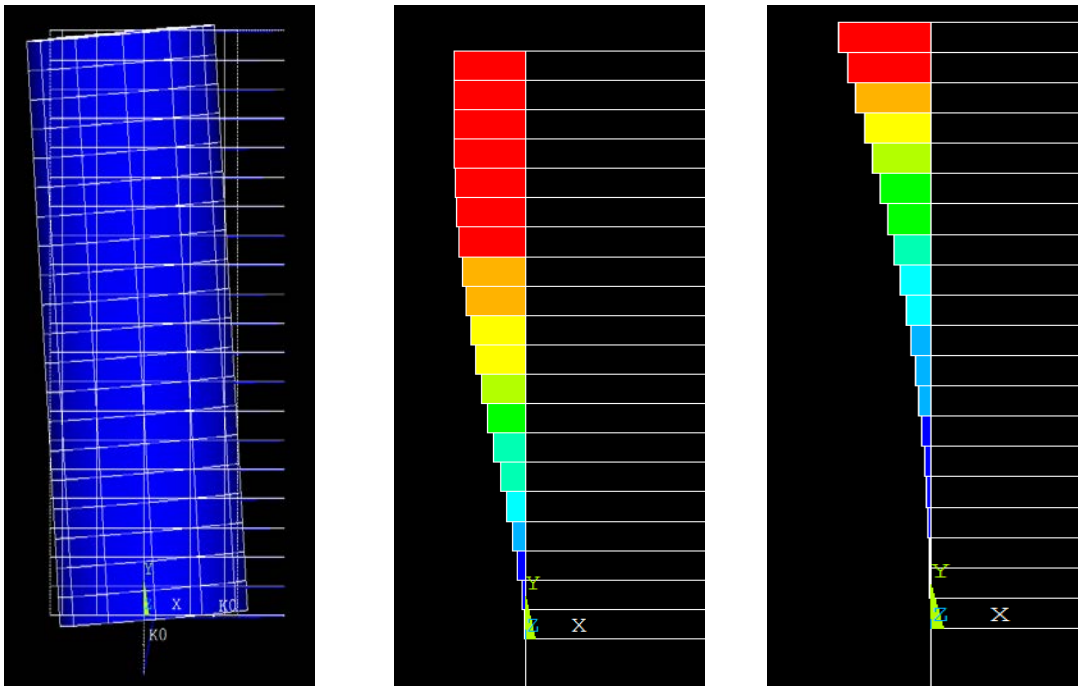
Table 5-12 Three-dimensional analysis model

Arm length size		
1.5 D removed	0.75 D removed	Cohesionless
50’-60’-70’-75’	50’-60’-70’-75’	50’-60’-70’-75’



(a) 3D displacement (b) M_y distribution (c) M_z distribution

Figure 5-9 50’ arm length in cohesive soil



(a) 3D displacement (b) M_y distribution (c) M_z distribution

Figure 5-10 50’ arm length in cohesionless soil

Table 5-13 3-dimension finite element analysis result in cohesive soil -0.75D removed

Arm length (ft)	Maximal M_y (kip-ft)	Maximal M_z (kip-ft)	Maximal Disp (ft)	Maximal rotation (Deg)
50	98.30	48.44	0.0308	0.0042
60	116.35	77.91	0.0410	0.0059
70	148.72	87.93	0.0510	0.0073
75	152.59	89.10	0.0530	0.0077

Table 5-14 3-dimension finite element analysis result in cohesive soil 1.5D removed

Arm length (ft)	Maximal M_y (kip-ft)	Maximal M_z (kip-ft)	Maximal Disp (ft)	Maximal rotation (Deg)
50	100.64	48.44	0.054	0.010
60	119.77	102.18	0.110	0.028
70	148.54	115.35	0.130	0.034
75	156.56	116.54	0.140	0.036

Table 5-15 3-dimension finite element analysis result in cohesionless soil

Arm length (ft)	Maximal M_y (kip-ft)	Maximal M_z (kip-ft)	Maximal Disp (ft)	Maximal rotation (Deg)
50	96.46	48.44	0.029	0.0047
60	113.9	67.42	0.034	0.0058
70	141.97	76.08	0.043	0.069
75	149.76	77.16	0.045	0.072

Chapter 6: Conclusion, Discussion, and Future work

6.1 Summaries and Conclusions

Finite element model has been demonstrated to be an effective approach to simulate shaft foundation of mast arm signal pole structure under linear range in the previous chapters. Results from analytical method should be more conservative but easy to obtain. Results based on finite element models should be more refined and accurate. This research findings can be made for shaft foundation design by comparing both of analyses methods.

[1] Based on general soil properties in Maryland, the existing design of shaft foundation can resist lateral force sufficiently. However, along with increasing arm length, required embedment lengths are close to the design lengths which means it is not allowed for additional load on superstructure.

[2] Torsional capacity is less than the torque induced by wind load in the worst case when the shaft foundation is installed in cohesionless soil. Thus, when wind reaches maximal speed, it is possible that foundation would fail due to superstructure horizontally rotation. To increase the torsional capacity, some shaft design would be strengthened by adding wing plate in the middle of shaft, which cost more and has been used for cantilever sign structures in Maryland.

[3] Broms' method currently adopted by the AASHTO LRFD Specifications (2015) can successfully cover maximal moment and its location. However, in the design procedure, the pile classification is not defined comprehensively. The structural behaviors of long pile and short pile are different. Thus, the size of shaft foundation such as the ratio of diameter and embedment length should be well-defined before analysis.

[4] The outcome from two-dimensional and three-dimensional models are consistent in either cohesive or cohesionless soils. Results from various dimensions of shaft are also consistent in two-dimensional and three-dimensional models. Therefore, three-dimensional model could be simplified by vector summing moments and shears along two horizontal axes as two-dimensional model in lateral reaction analysis, except handling torsion.

[5] For cohesive soil, neglecting soil reaction of 1.5 pile diameter in depth in the short free head pile is conservative for signal pole foundation. In the current case, the embedment length of shaft foundation is 10 feet and its diameter is 4 feet. If Broms' assumption is adopted for this case, more than 50% shaft (6') would not laterally restrained. From finite element analysis, the restrain of shaft seems too loosely fixing the shaft body; therefore, shaft body resist more moment than expected.

[6] The lateral reaction performance of the three-dimensional model assigned with all external loads seems less conservative than Broms' analytical method. Therefore, foundation designed based on the current AASHTO design specifications would covers lateral soil reaction capacity even considering the torsional effect.

6.2 Future work

The goal of this study is to verify current shaft foundation design for mast arm signal pole structure by analytical method and finite element method in the static stage under linear range. By validating finite element model accuracy, non-linear interaction between soil and shaft could be further developed with nonlinear p-y curve based on effective finite element models. When extreme case occurs, such as tornado and hurricane, it would facilitate state administration to evaluate safety and capability of signal pole structures more efficiently since foundation is generally invisible and hardly detectable.

Bibliography

AASHTO LRFD Specification for Structural Supports for Highway Signs, Luminaires, and Traffic Signals, 2015

Broms, M., Lateral Resistance of Piles in Cohesive Soils. Journal of the Soil Mechanics and Foundations Division © ASCE / March 1964

Broms, M., Lateral Resistance of Piles in Cohesionless Soils. Journal of the Soil Mechanics and Foundations Division © ASCE / May 1964

Coduto, Donald P., Foundation Design Principles and Practice Second Edition, 2001, ISBN 0-13-589706-8

Davisson, M. T., Lateral Load Capacity of Piles. Department of Civil Engineering, University of Illinois, Urbana, 1970

Drilled Shafts: Construction Procedures and LRFD Design Methods, NHI Course No. 132014, FHWA, May,2010

Florida Bridge Software Institute, FB-MultiPier Version 5.1.1, 2011

Greimann, Lowell and Wolde-Tinsae, Amde M., Design Model for Piles in Jointless Bridges. ASCE, 1988

Heyery, Barry J. and Reese, Lymon C., Analysis of Single Piles under Lateral Loading. FHWA/TX-79/38+244-l, December 1979

Hu, Zhihong, Determining the Optimum Depth of Drilled Shafts Subject to Combined Torsion and Lateral Loads in Saturated Sand from Centrifuge Testing, 2003

Murthy, V.N.S, Geotechnical Engineering Principles of Soil Mechanics and Foundation Engineering,2003, ISBN 0-8247-0873-3

Nusairat, Jamal et al., Drilled Shaft Design for Sound Barrier Walls, Signs, And Signals, 2004

Recommended Practice for Planning, Designing and Constructing Fixed Offshore Platforms—Working Stress Design. API, 2005

Ruigrok, J.A.T, Laterally Loaded Piles Models and Measurements, 2010

Stuedlein, Armin W. et.al, Evaluation of Torsional Load Transfer for Drilled Shaft Foundations Final Report, SPR 304-701, 2016